International Journal of High-Rise Buildings
December 2020, Vol 9, No 4, 315-323
https://doi.org/10.21022/IJHRB.2020.9.4.315

International Journal of
High-Rise Buildings
www.ctbuh-korea.org/ijhrb/index.php

Seismic Capacity Required for the Safety Limit Design of High-rise RC Buildings under Long-period Ground Motions in Osaka, JAPAN and its Estimation Based on the Equivalent Linearization Method

Yasushi Sanada[1], Hiroki Yoshida[1], and Masayuki Awano[2]

[1]*Department of Architectural Engineering, Osaka University, Japan*
[2]*Department of Architecture, Kindai University, Japan*

Abstract

In June 2016, the Ministry of Land, Infrastructure, Transport and Tourism (MLIT) in Japan delivered countermeasures against long-period ground motions caused by strong earthquakes along the Nankai trough. However, the countermeasures do not cover high-rise buildings equal to or shorter than 60 m in height, which do not require earthquake response analyses in the seismic design. Hence, in the present study, earthquake response analyses for such high-rise reinforced concrete (RC) buildings were performed under artificial ground motions assumed in the OS1 and OS2 regions to determine the base shear coefficients that satisfy a given safety demand. Furthermore, the results from the earthquake response analyses were estimated by the authors' proposed method based on the equivalent linearization method, showing good agreement and inspiring suggestions for more accurate and simplified estimations.

Keywords: Earthquake response analysis, Equivalent linearization method, Hysteretic damping, Long-period ground motion, Reinforced concrete

1. Introduction

In June 2016, the Ministry of Land, Infrastructure, Transport and Tourism (MLIT) in Japan delivered countermeasures against the long-period ground motions caused by strong earthquakes along the Nankai trough in the form of technical advice considering the lessons learned from the 2011 Tohoku earthquake (MLIT, 2016). However, the countermeasures do not cover high-rise buildings equal to or lower than 60 m in height that do not require earthquake response analyses for seismic design in Japan (only super high-rise buildings higher than 60 m in height are covered). Hence, in this study, earthquake response analyses for such high-rise reinforced concrete (RC) buildings were performed under the artificial ground motions assumed in the OS1 and OS2 regions that were defined in the technical advice, shown in Figure 1, to evaluate the base shear coefficients that satisfy the safety demands, shown in Table 1, provided by the Japan Structural Consultants Association (JSCA) (Kitamura et al., 2006). Furthermore, an estimation method for the required base shear coefficients based on the equivalent linearization method was proposed in the present study and was applied to practically evaluate the results from the earthquake response analyses.

†Corresponding author: Yasushi Sanada
Tel: +81-6-6879-7637
E-mail: sanada@arch.eng.osaka-u.ac.jp

2. Analytical Structures

The present study focuses on regular high-rise RC buildings with different numbers of stories: 12, 14 and 16. The total building heights were 42 m, 49 m and 56 m for the 12-, 14- and 16-story models, respectively, where each story height was 3.5 m. The span lengths were 7 m and 10 m in the longitudinal and transverse directions, respectively. The analytical models represented the interior one-span moment-resisting frames in the longitudinal direction, as shown in Figure 2; namely, the frames were replaced by plane fishbone models. A unit floor weight of 12 kN/m^2 was assumed for the following structural design and analyses.

The column width and depth of each model were common over the height. Different design compression strengths of concrete F_c were assumed for every four stories so that the axial force ratios (the applied axial force/column compressive strengths) were within approximately 0.15. The beam width and depth were designed to satisfy equation (1) from the design standards of the Architectural Institute of Japan (AIJ, 2018).

$$l/D = \sqrt{C_c b/\alpha\omega_0} \tag{1}$$

where l: the beam span length, D: the beam depth, C_c: 0.6 N/mm^2 for a rectangular beam section, b: the beam width, α: 1/16 for beams fixed at both ends, and w_0: the average

Table 1. Standards for seismic performance

Target	Performance evaluation items	Safety limit level III	Safety limit beyond level III
Building response	Story drift angle (rad)	1/100~1/75	1/75~
	Floor acceleration ($\times 10^{-2}$ m/s^2)	500~1000	1000~
Structural member	Ductility factor μ	3.75~5.0	5.0~

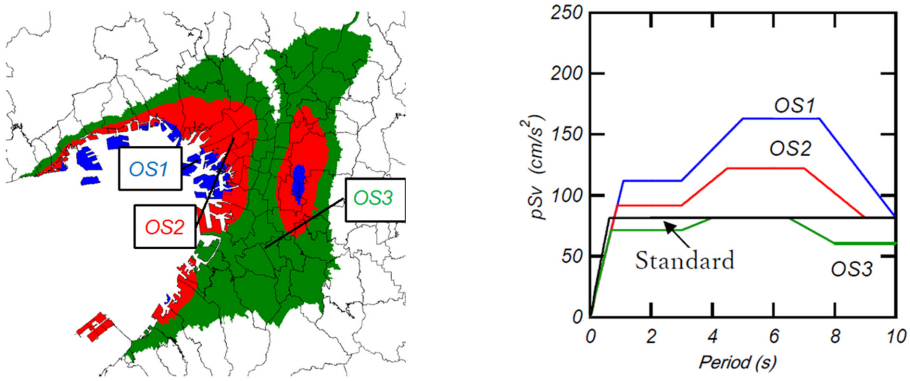


Figure 1. Regional map of Osaka and the seismic design spectra for long-period ground motions (MLIT, 2016).

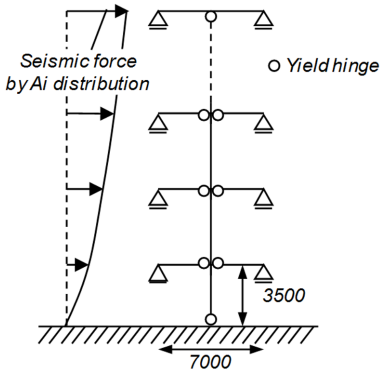


Figure 2. Analytical model. (unit: mm)

vertical load per unit length.

The cross-sectional dimensions of the columns and beams designed according to the above concept are listed in Table 2. The elastic vibration characteristics of all models were calculated as shown in Table 3.

The interstory beam flexural strengths were designed so that the story shear coefficient C_i (BCJ, 2016) from equation (2) was satisfied for every story under a design parameter of D_s ranging from approximately 0.3 (which is the minimum value for the typical ductile design of RC buildings in Japan) to 0.9 at intervals of 0.005. The column flexural strengths at the bottom and rooftop were similarly designed, while the beams at the rooftop and

Table 2. Summary of the analytical models

12-story models (height = 42 m)		1F-4F	5F-8F	9F-12F	
		F_c = 56 N/mm^2	F_c = 38 N/mm^2	F_c = 24 N/mm^2	
Column	Cross section (mm)		1100x1100		
	Axial force ratio	0.150 (1F)	0.146 (5F)	0.116 (9F)	
Beam	Width x depth (mm)	700 × 1050	700 × 1000	700 × 950	
14-story models (height = 49 m)		1F-4F	5F-8F	9F-12F	13F-14F
		F_c = 60 N/mm^2	F_c = 42 N/mm^2	F_c = 27 N/mm^2	F_c = 24 N/mm^2
Column	Cross section (mm)		1150x1150		
	Axial force ratio	0.150 (1F)	0.151 (5F)	0.141 (9F)	0.053 (13F)
Beam	Width x depth (mm)	700 × 1100	700 × 1050	700 × 1000	700 × 950
16-story models (height = 56 m)		1F-4F	5F-8F	9F-12F	13F-16F
		F_c = 60 N/mm^2	F_c = 48 N/mm^2	F_c = 32 N/mm^2	F_c = 24 N/mm^2
Column	Cross section (mm)		1200x1200		
	Axial force ratio	0.160 (1F)	0.146 (5F)	0.146 (9F)	0.097 (13F)
Beam	Width x depth (mm)	700 × 1100	700 × 1050	700 × 1000	700 × 950

Table 3. Elastic vibration characteristics

Analytical model	Primary natural period (s)	Primary equivalent mass ratio (%)
12-story model	0.89	78.0
14-story model	0.97	77.2
16-story model	1.09	76.7

interstory column were designed with flexural strengths twice those of the adjacent column and beams, respectively, to form an overall collapse mechanism, as shown in Figure 2. As a result, multiple models with different D_s were prepared for the 12-, 14- and 16-story models.

$$C_i=(Z\times R_t\times A_i\times C_0)\times D_s\times F_{es} \quad (2)$$

where Z: a regional factor (= 1.0), R_t: a vibration characteristic factor (= 0.997, 0.991, and 0.973 for the 12-, 14- and 16-story models under soft soil conditions), A_i: the distribution of the design story shear coefficients along the building height, C_0: the standard design base shear coefficient (= 1.0), D_s: a reduction factor for C_0 considering the inelastic drift capacity, and F_{es}: an amplification factor for C_0 considering the structural irregularity (= 1.0).

The elastic modulus of the concrete was calculated according to the AIJ design standards (AIJ, 2018).

3. Earthquake Response Analysis

3.1. Modeling and Numerical Methods

Time history earthquake response analyses were performed on the above models under artificial long-period ground motions in the OS1 and OS2 regions to evaluate the base shear coefficients of ${}_{res}C_b$ that satisfy the safety demand of the maximum interstory drift angle of 1/75 rad, presented in Table 1. Within the present study, however, the other items in Table 1 were not considered because the interstory drift angle is the most common safety demand in practical structural design in Japan.

The plane fishbone moment-resisting frame models shown in Figure 2 were used for the analyses. The first-story column bottom was fixed, and rigid floors were assumed. Each beam/column was replaced by a line element that considered the inelastic bending and elastic shear/axial behavior. A rigid zone with a quarter of the beam/column depth was also considered at each joint end of the line element. Figure 3 illustrates the skeleton curves and hysteresis rules of the Takeda model (Takeda et al., 1970) applied to the beams and columns. The bending moment at cracking M_c was assumed to be a quarter of the flexural strength at yielding M_y. The secant stiffness at yielding K_2 was assumed at a quarter of the elastic stiffness K_1 (α_y = 0.25 in the figure) of the model with a standard D_s of 0.3, while the drift angle at yielding θ_y obtained from the above standard model was constant for the other models with higher D_s.

Newmark's β method was applied for numerical integration, with a β of 0.25. The viscous damping was assumed to be proportional to the secant stiffness, with a damping ratio of 5%.

3.2. Long-Period Ground Motions

Two artificial ground motions in the OS1 and OS2 regions were generated based on the countermeasures by MLIT, Japan, in June 2016 which included the seismic design spectra on the engineering bedrock shown in Figure 1. Figure 4 shows the acceleration time histories of the two ground motions, which were calculated with

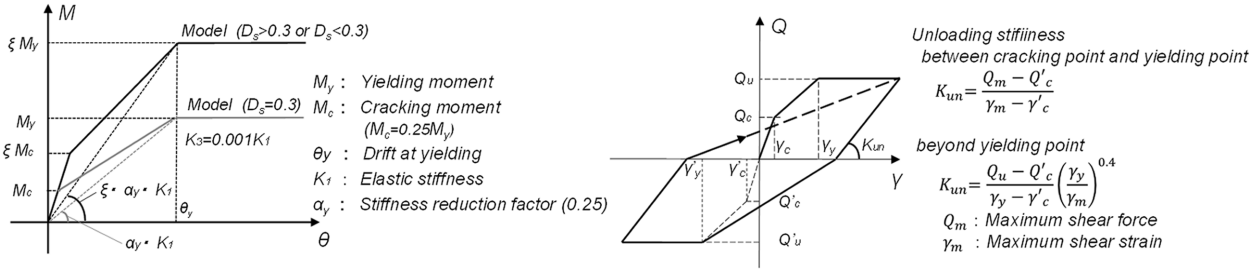


Figure 3. Restoring force characteristics and the hysteretic model.

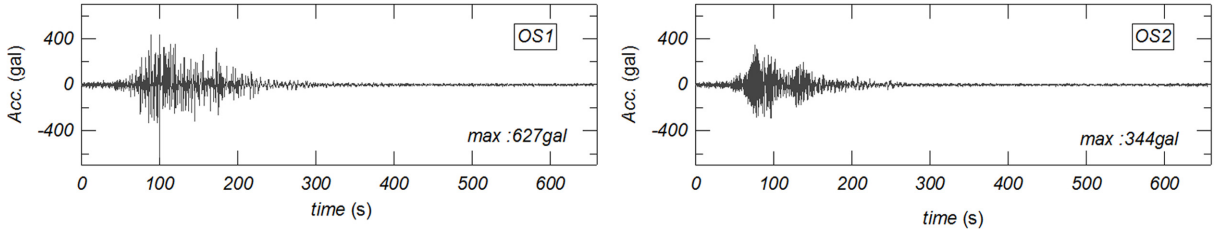


Figure 4. Ground acceleration time histories of the artificial waves.

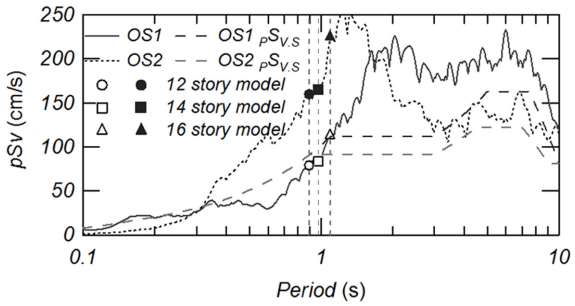


Figure 5. Pseudo velocity response spectra.

actual surface ground conditions in the OS1 and OS2 regions. Figure 5 shows the spectral velocity responses with the elastic fundamental periods of the 12-, 14- and 16-story models, and the design spectra on the engineering bedrock are shown in Figure 1.

3.3. Analytical Results

Figure 6 shows the maximum interstory drift responses of the representative models with different D_s of 0.3, 0.4, 0.5 and 0.6, and the safety limit of the maximum interstory drift angle of 1/75 rad is also indicated in the figure. Focusing on the OS1 ground motion, the interstory drift responses decreased with increasing D_s for all the groups of models with different numbers of stories. Similar interstory drift profiles along the height were observed for the models with D_s equal to/higher than 0.5. The drift responses were generally within the safety limit. On the other hand, the OS2 ground motion amplified the interstory drift responses at the upper/lower floors in the cases with D_s of 0.3 and higher to beyond the safety limit. Within the analytical conditions in this study, the OS2 ground motion was likely to cause more severe drift responses for high-rise RC buildings.

Figure 7 extracts the profiles with a maximum interstory drift angle of approximately 1/75 rad. In the case of the OS1 ground motion, the minimum D_s values satisfying the safety limit were 0.255, 0.280 and 0.280 for the 12-, 14- and 16-story models, respectively. In contrast, much higher D_s values of 0.620, 0.575 and 0.685 were required for the 12-, 14- and 16-story models, respectively, under the OS2 ground motion. Table 4 summarizes the base shear coefficients ${}_{res}C_b$ required to satisfy the safety limit under both ground motions based on equation (2) and the above results. In practical structural design in Japan, however, earthquake response analysis is not commonly performed; thus, these requirements need to be estimated in some alternative way. This study adopts the equivalent linearization method (e.g. ATC, 1996) and discusses the

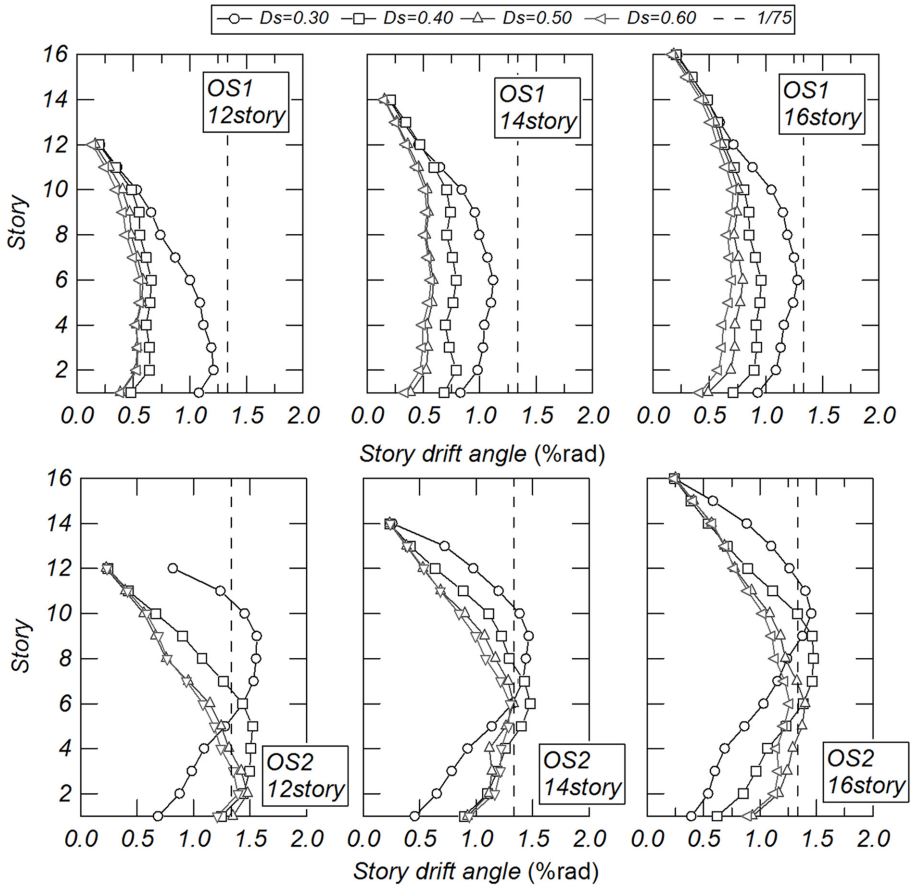


Figure 6. Profiles of the maximum interstory drift angles.

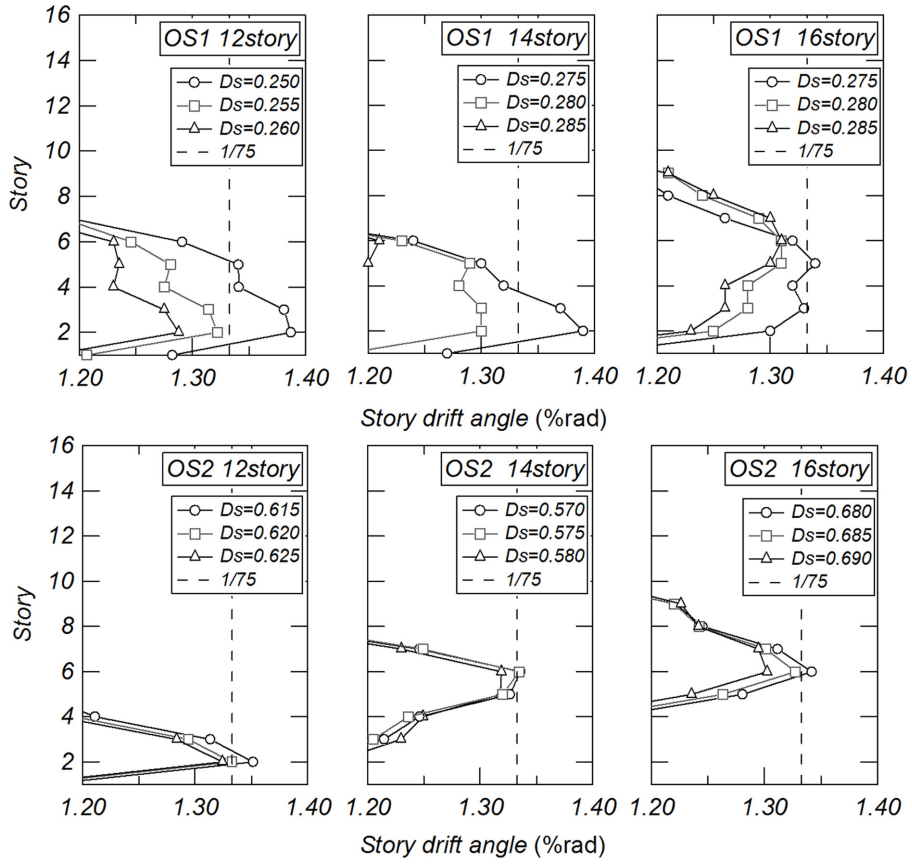


Figure 7. Profiles of the maximum interstory drift angles (magnification of app. 1/75 rad).

Table 4. Required base shear coefficients (earthquake response analysis)

${}_{res}C_b$	12 story	14 story	16 story
OS1	0.254	0.277	0.272
OS2	0.618	0.570	0.667

estimation accuracy as follows.

4. Estimation of the Required Base Shear Coefficients Based on the Equivalent Linearization Method

4.1. Proposal of an Estimation Procedure

The earthquake responses of the analytical models under the OS1 and OS2 ground motions were evaluated through the time history response analyses in the previous section. As mentioned in the introduction of the present paper, however, high-rise buildings equal to or shorter than 60 m in height do not require earthquake response analyses for seismic design in Japan. Therefore, this study focuses on an equivalent linearization method for estimating the results from earthquake response analyses, in particular, the base shear coefficients ${}_{res}C_b$ required to satisfy the safety limit shown in Table 4. The estimation procedure proposed in this study is illustrated in Figure 8. The

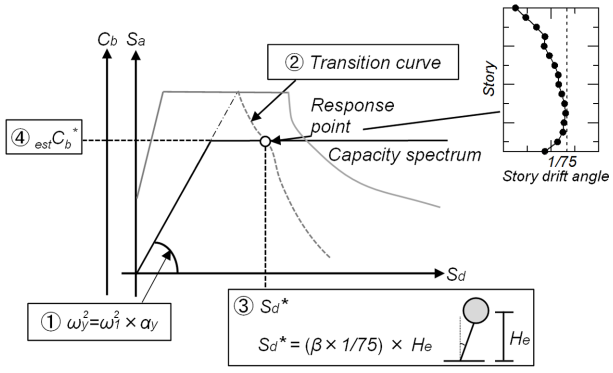


Figure 8. Procedure proposed for estimating the base shear coefficient requirements.

equivalent linearization method enables the estimation of the maximum earthquake response of a building by finding an intersection between the capacity spectrum (the S_a-S_d relationship representing the capacity curve of the equivalent single-degree-of-freedom system, which is replaced by the bilinear model) and the demand spectrum of the ground motion (the S_a-S_d relationship representing the spectral response acceleration and drift), as shown in Figure 8. The step-by-step estimation procedure is as follows (the numbers for the following steps are consistent with those in Figure 8):

Step 1: The secant stiffness at the yield point ω_y^2 is calculated by equations (3) to (5).

$$T_1 = 0.02H \tag{3}$$

$$\omega_1 = \frac{2\pi}{T_1} \tag{4}$$

$$\omega_y^2 = \omega_1^2 \times \alpha_y \tag{5}$$

where H: the building height (m), T_1: the elastic fundamental period, ω_1: the elastic fundamental circular frequency, and α_y: the ratio of the secant stiffness at yield to the elastic stiffness.

Step 2: The transition curve representing the inelastic responses beyond the yield point is calculated based on ω_y^2 from equation (5), which is obtained by multiplying the demand spectrum beyond the yield point by the response reduction factor F_h from equations (6) and (7). F_h from equation (7) is commonly used for the performance-based design of RC buildings in Japan (AIJ, 2019).

$$h = 0.25\left(1 - \frac{1}{\sqrt{\mu}}\right) + 0.05 \tag{6}$$

$$F_h = \frac{S(h)}{S(h=0.05)} = \frac{1.5}{1+10h} \tag{7}$$

where h: the damping ratio considering the inelastic hysteretic energy dissipation and μ: the ratio of the maximum drift beyond the yield point to the yield drift.

Step 3: The maximum drift capacity satisfying the safety limit (an interstory drift angle of 1/75 rad in this study) of the single-degree-of-freedom system S_d^* is calculated by equation (8).

$$S_d^* = H_e \times \left(\frac{1}{75} \times \beta\right) \tag{8}$$

where H_e is the representative height of the building and β is the ratio of the drift at the representative height to the interstory drift of 1/75 rad.

Step 4: The capacity spectrum is determined such that the maximum drift response (S_d at the intersection of the capacity spectrum and the transition curve) is within the safety limit S_d^*. The base shear coefficient ${}_{est}C_b^*$ required to satisfy the safety limit is estimated by equation (9) with S_a at the intersection.

$${}_{est}C_b^* = \frac{S_a}{g} \times \frac{M_e}{M_t} \tag{9}$$

where g: the gravity acceleration, M_e: the effective mass of the single-degree-of-freedom system, and M_t: the building total mass.

4.2. Application and Results

The required base shear coefficients ${}_{res}C_b$ from the earthquake response analyses shown in Table 4 were estimated according to the proposed procedure shown in Figure 8. However, the capacity spectrum was obtained from a pushover analysis of each analytical model (Section 3.1) by applying equations (10) and (11) and was then represented by a bilinear relationship with the equivalent enclosed area. Thus, within the present study, the two factors α and β related to the capacity spectrum were regressively evaluated for future application to practical design. Additionally, the demand spectra were evaluated based on the time history data of the OS1 and OS2 ground motions (Figure 4) and are shown in Figure 9.

$$S_a = \frac{\sum_{i=1}^{N} m_i \delta_i^2}{\left(\sum_{i=1}^{N} m_i \delta_i\right)^2} Q_B \tag{10}$$

$$S_d = \frac{\sum_{i=1}^{N} m_i \delta_i^2}{\sum_{i=1}^{N} P_i \delta_i} S_a \tag{11}$$

where m_i: the mass of the i-th floor, δ_i: the lateral drift at

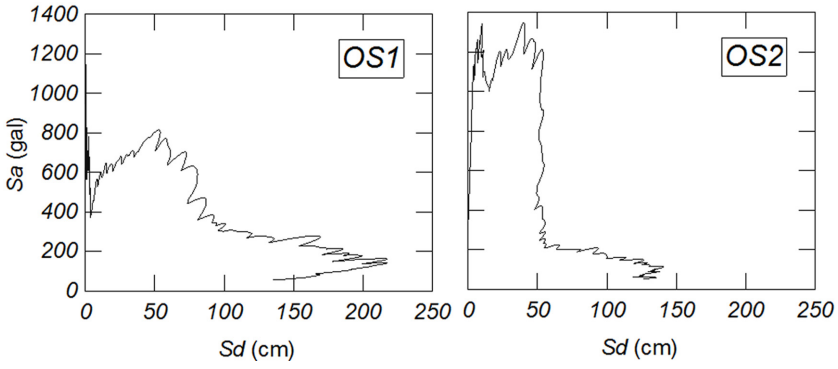


Figure 9. Demand spectra with 5% damping.

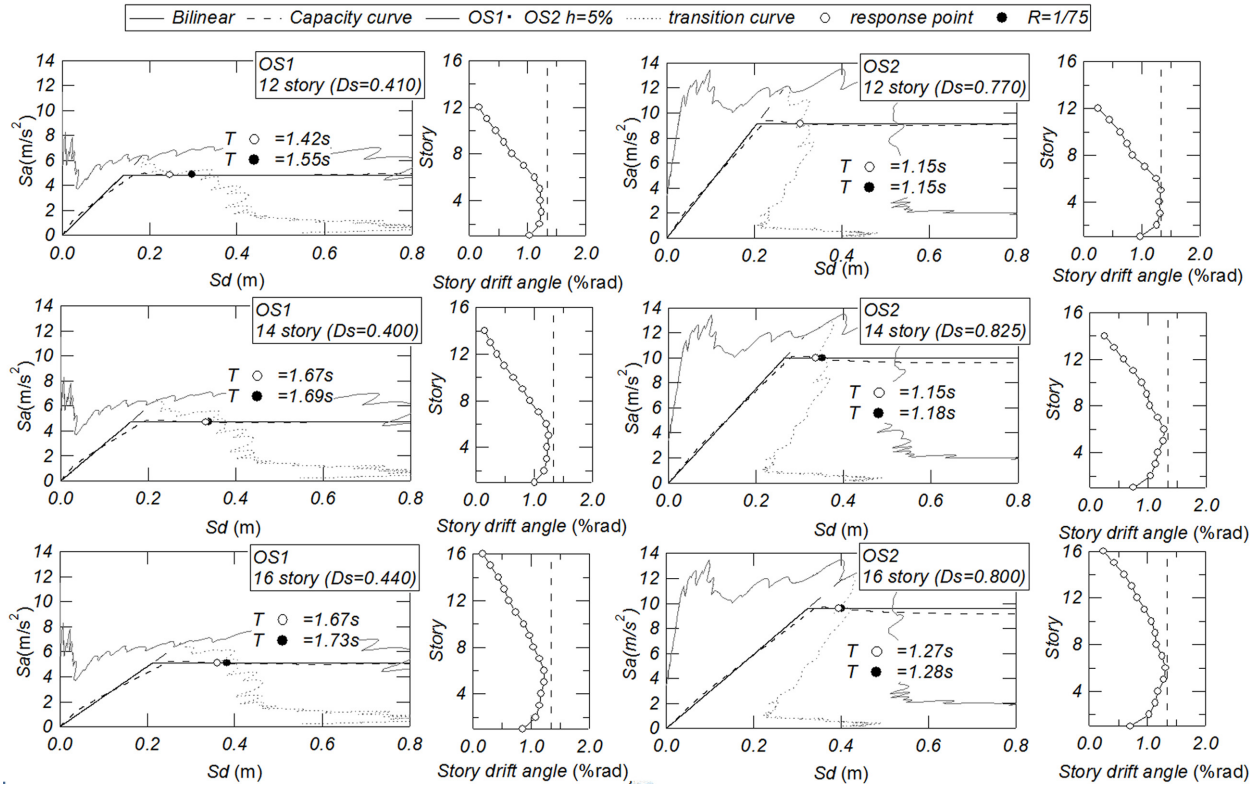


Figure 10. Response point evaluation results.

the i-th floor, P_i : the seismic force (lateral load) applied to the i-th floor, and Q_B : the base shear force.

Figure 10 illustrates the estimation results for all the models under the OS1 and OS2 ground motions, where the white and black circles represent each estimated response and a step in the pushover analysis when the maximum interstory drift angle of 1/75 rad is initially observed. Table 5 summarizes the estimated base shear coefficients ${}_{est}C_b^*$ required to satisfy the safety limit compared to those (${}_{res}C_b$) from the earthquake response analyses in Table 4. In general, the estimation results exceeded those from the earthquake response analyses, which was due to the large gaps between the analyzed and estimated inelastic response reduction factors. Figure 11 compares the inelastic response reduction factors from the response drift spectra with different damping ratios for the OS1 and OS2 ground

Table 5. Estimated required base shear coefficients

OS1	${}_{est}C_b^*$	${}_{res}C_b$	${}_{est}C_b^*/{}_{res}C_b$	OS2	${}_{est}C_b^*$	${}_{res}C_b$	${}_{est}C_b^*/{}_{res}C_b$
12 story	0.403	0.254	1.59	12 story	0.757	0.618	1.22
14 story	0.392	0.277	1.41	14 story	0.803	0.570	1.41
16 story	0.418	0.272	1.54	16 story	0.764	0.667	1.15

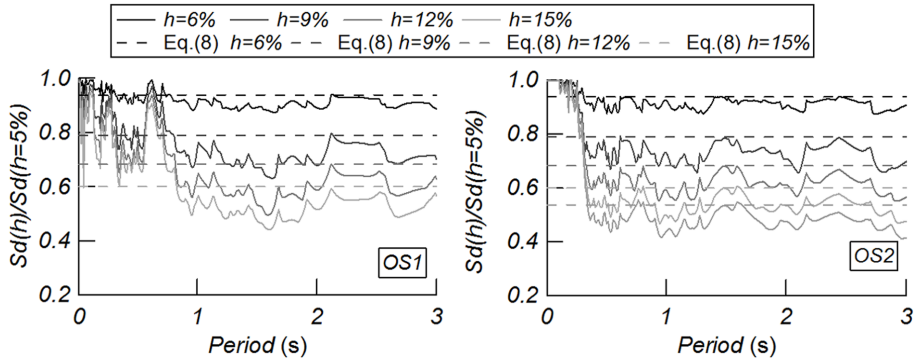


Figure 11. Equation (7) vs. the spectral response reduction factors.

motions, represented by solid lines, with the estimations for F_h from equation (7), represented by dotted lines. The equation clearly underestimated the inelastic response reduction factors from the analyses, yielding overestimations for the required base shear coefficients, as shown in Table 5.

4.3. Modification for Better Accuracy

To modify the estimation accuracy, the present study focused on the modified equation (12) for F_h by Kobayashi et al., which was proposed for long-period ground motions caused by strong earthquakes along the Nankai trough, replacing equation (7), the equation commonly used for performance-based design in Japan (AIJ, 2019).

$$F_h = \frac{1+\alpha h_0}{1+\alpha h} \tag{12}$$

where h_0: the initial damping ratio and α: a regression coefficient. The above equation was appropriate for the case where the fundamental period of the building was shorter than the corner period of 3 s in the spectra of Figure 1 (refer to the citation for other cases). In addition, the regression coefficient was evaluated for base isolated buildings in the reference (Kobayashi et al., 2019); thus, the regression coefficient was re-evaluated for high-rise RC buildings in the present study as follows:

- The regression analyses were performed for periods between 0.89 s and 2.21 s, which represented the shortest fundamental period of the 12-story model and the longest equivalent period observed in all cases in the earthquake response analyses, respectively.
- The range of the response reduction factors was represented by those where h = 0.06 to 0.17. The upper limit of 0.17 was approximately consistent with the maximum from equation (6) observed for all the cases in the earthquake response analyses.

As a result, the regression coefficient of α was 19.8/16.1 for the OS1/OS2 ground motions. Figure 12 recompares the response reduction factors from the response drift spectra shown in Figure 11 with the estimations for F_h from equation (12), showing the improvements in the agreements between the two. Furthermore, Table 6 compares the re-estimated base shear coefficients required to satisfy the safety limit with those from the earthquake response analyses in Table 4. The estimation accuracy was much better after the application of equation (12) with the above regression coefficients representing the characteristics of the long-period ground motions.

In addition, within the analytical results obtained in the present study, the ratio of the secant stiffness at yield to the elastic stiffness α_y and the ratio of the drift at the representative height to the interstory drift of 1/75 rad β in the proposed estimation procedure of Figure 8 are discussed for future application to practical design. Figure 13 shows the relationships between α_y and D_s from equation (2), which is the major design parameter of the analytical

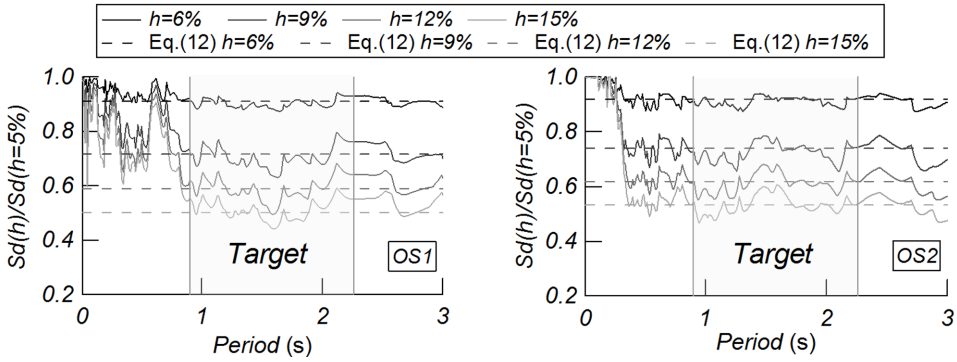


Figure 12. Equation (12) vs. the spectral response reduction factors.

Table 6. Re-estimation of the required base shear coefficients

OS1	${}_{est}C_b^*$	${}_{res}C_b$	${}_{est}C_b^* / {}_{res}C_b$	OS2	${}_{est}C_b^*$	${}_{res}C_b$	${}_{est}C_b^* / {}_{res}C_b$
12 story	0.326	0.254	1.28	12 story	0.611	0.618	0.99
14 story	0.290	0.277	1.05	14 story	0.653	0.570	1.15
16 story	0.280	0.272	1.03	16 story	0.734	0.667	1.10

Table 7. List of β from equation (8)

OS1	H_e (m)	S_d^* (m)	β	OS2	H_e (m)	S_d^* (m)	β
12 story	28.08	0.294	0.785	12 story	28.31	0.303	0.802
14 story	32.59	0.340	0.782	14 story	33.09	0.347	0.786
16 story	37.41	0.383	0.768	16 story	38.05	0.400	0.788

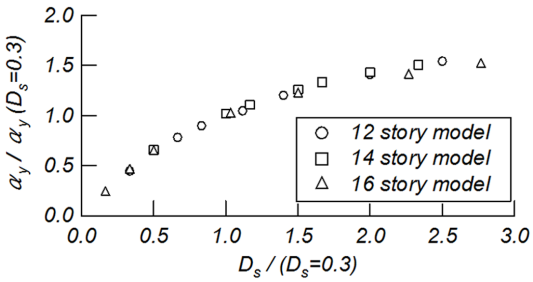


Figure 13. Scatter plot of α_y from equation (5).

structures, as explained in Section 2; however, both are standardized by the values of the standard case with D_s of 0.3. A trend was exhibited where α_y gradually increased with increasing D_s, indicating higher lateral resistance, which was likely attributed to the modeling assumption with constant θ_y in Figure 3. Table 7 summarizes the β values of each analytical model listed in Table 6, which were regressively evaluated from equation (8) and the pushover analysis. The range of β was relatively narrow, at approximately 0.8.

5. Conclusions

The present study investigated the base shear coefficients of high-rise (12-, 14- and 16-story) RC buildings required to reduce the maximum interstory drift response to within the safety limit of 1/75 rad through earthquake response analyses under two designed long-period ground motions in the OS1 and OS2 regions, Osaka, Japan. Furthermore, an estimation method for the required base shear coefficients based on the equivalent linearization method was proposed and applied to practically evaluate the results from the earthquake response analyses. The major findings from the present research are summarized as follows:

1. The base shear coefficients required for the OS1 ground motion were less than 0.3, which is approximately the minimum requirement for the safety limit design of ductile moment-resisting frame structures in Japan. In contrast, those for the OS2 ground motion were very high, exceeding 0.55, which is commonly applied to nonductile lateral force-resisting wall structures in Japan.
2. The equivalent linearization method was applied to estimate the results from the earthquake response analyses. The procedure of the proposed estimation method is illustrated in the present paper. Consequently, it was found that inelastic response reduction under hysteretic damping was a key issue for precise estimation; thus, the method under long-period ground motions was modified based on the proposal by Kobayashi et al. (2019), which improved the accuracy of the estimation.
3. The two factors α_y and β from the capacity spectrum needed for the estimation procedure were regressively evaluated, which are continuously discussed for future application of the procedure to practical design.

As mentioned above, within the present study, the OS2 ground motion was much more severe than the OS1 ground motion regarding the seismic design of high-rise RC buildings. The proposed estimation scheme is likely to contribute to evaluate the design base shear coefficient differently required at each construction site. However, these results might be attributed to the surface soil amplifying the ground motions; thus, further study is needed to clarify the generality of the above results. Furthermore, for application to practical design, the formulation of the demand and capacity spectra should be simplified in future studies.

6. Acknowledgments

This study was performed as a part of the activities of the RC committee of the AIJ Kinki branch. The long-period ground motions for the analyses were provided by the committee members. The authors deeply appreciate their kind support. This study was also financially supported by the JSPS KAKENHI grant number 20H00275.

References

Applied Technology Council (ATC). (1996) ATC-40 Seismic Evaluation and Retrofit of Concrete Buildings Volume 1. Report No. SSC 96-01.

Architectural Institute of Japan (AIJ). (2018) Standard for Structural Calculation for Reinforced Concrete Structures (in Japanese).

Architectural Institute of Japan (AIJ). (2019) AIJ Seismic Performance Evaluation Guidelines for Reinforced Concrete Buildings Based on the Capacity Spectrum Method (in Japanese).

Building Center of Japan (BCJ) (2016) The Building Standard Law of Japan.

Kitamura, H., Miyauchi, Y. and Uramoto, H. (2006) Study on Standards for Judging Structural Performances in Seismic Performance Based Design -Evaluation of the safety limit value and margin I and II levels in JSCA seismic performance menu- (in Japanese). *Journal of Structural and Construction Engineering* (Transactions of AIJ), 604, 183-191.

Kobayashi, M. and Kataoka, Y. (2019) A Proposal of Damping Correction Formula Considering Period-Dependent Characteristics of the Design Response Spectra of Long-Period Ground Motions for the Hypothetical Nankai Trough Earthquake (in Japanese), *Journal of Structural and Construction Engineering* (Transactions of AIJ), No. 758, pp. 477-487.

Ministry of Land, Infrastructure, Transport and Tourism (MLIT) (2016) https://www.mlit.go.jp/jutakukentiku/build/jutakukentiku_house_fr_000080.html (in Japanese)

Takeda, T., Sozen, M.A. and Nielsen, N.M. (1970) Reinforced concrete response to simulated earthquakes. *Journal of Structural Division*, ASCE, 96(ST12), 2557-2573.